

Seismic damage assessment of steel reinforced recycled concrete column-steel beam composite frame joints

Jing Dong¹, Hui Ma^{*1,2}, Nina Zhang¹, Yunhe Liu^{1,2} and Zhaowei Mao¹

¹School of Civil Engineering and Architecture, Xi'an University of Technology, Xi'an, China

²State Key Laboratory of Eco-hydraulic Engineering in Arid Area, Xi'an University of Technology, Xi'an, China

(Received June 23, 2017, Revised January 22, 2018, Accepted January 28, 2018)

Abstract. Low cyclic loading tests are conducted on the steel reinforced recycled concrete (SRRC) column-steel (S) beam composite frame joints. This research aims to evaluate the earthquake damage performance of composite frame joints by performing cyclic loading tests on eight specimens. The experimental failure process and failure modes, load-displacement hysteresis curves, characteristic loads and displacements, and ductility of the composite frame joints are presented and analyzed, which shows that the composite frame joints demonstrate good seismic performance. On the basis of this finding, seismic damage performance is examined by using the maximum displacement, energy absorbed in the hysteresis loops and Park-Ang model. However, the result of this analysis is inconsistent with the test failure process. Therefore, this paper proposes a modified Park-Ang seismic damage model that is based on maximum deformation and cumulative energy dissipation, and corrected by combination coefficient α . Meanwhile, the effects of recycled coarse aggregate (RCA) replacement percentage and axial compression ratio on the seismic damage performance are analyzed comprehensively. Moreover, lateral displacement angle is used as the quantification index of the seismic performance level of joints. Considering the experimental study, the seismic performance level of composite frame joints is divided into five classes of normal use, temporary use, repair after use, life safety and collapse prevention. On this basis, the corresponding relationships among seismic damage degrees, seismic performance level and quantitative index are also established in this paper. The conclusions can provide a reference for the seismic performance design of composite frame joints.

Keywords: steel reinforced recycle concrete columns; steel beams; joints; seismic performance level; seismic damage model

1. Introduction

Rapid urbanisation has caused many negative problems, such as exploitation of nonrenewable natural resources and production of large amounts of construction waste (Leiva *et al.* 2013, Matar and Dalati 2011, Radonjanin *et al.* 2013, Kumar 2017). The introduction and research of the recycled aggregate concrete (RAC) can provide an effective way to solve these problems effectively. In the RAC material, the recycled coarse aggregate (RCA) can replace the natural coarse aggregate (NCA) partly or totally. RCA is a green construction material that can contribute to the sustainable development of the concrete industry. A considerable amount of experimental studies have been conducted on the material properties and structural behaviour of RAC (Carneiro *et al.* 2014, Wagih *et al.* 2013, Choi and Yun 2012, Manzi *et al.* 2013, Thomas *et al.* 2013, Silva *et al.* 2016, Kou *et al.* 2012, Mas *et al.* 2012, Xiao *et al.* 2012). Their results show that the main mechanical properties of RAC material, such as compression strength, elastic modulus and durability are generally lower than those of conventional concrete due to the adhesion of old mortar and

aging of aggregates in RCA. Although the mechanical properties of RAC are inferior to those of ordinary concrete, RAC can still be applied in structures as long as the mixture ratio design and construction details are appropriate.

Steel reinforced recycled concrete (SRRC) refers to a kind of steel and RAC composite structures that are equipped with a profile steel, longitudinal rebars and transverse stirrups. It not only has the advantages of high bearing capacity and good seismic performance of the ordinary steel and concrete composite structures, but also has the characteristics of energy conservation and environmental protection. Popularization and application of RAC are significant and important. In the previous study (Ma *et al.* 2013), the results show that the SRRC columns under cyclic loading demonstrate good seismic performance and high bearing capacity. In addition, the joint is the key part of connecting beams and columns in frame structure. Therefore, it is necessary to study the mechanical performance of composite frame joints. The seismic performance and shearing strength of SRRC beam-SRRC column frame joints were studied by literature (Xue *et al.* 2014), which revealed that these joints exhibit good seismic performance, but their construction is highly complicated and inconvenient in practical engineering.

Given this background, a new type of hybrid structure called steel-reinforced recycled concrete column-steel beam (SRRC column-S beam) composite frame joint was

*Corresponding author, Ph.D.
E-mail: mahuiwell@163.com

Table 1 Design parameters of specimens

Specimen No.	RAC strength grade	Axial compression ratio n	RCA replacement percentage $r/\%$	Profile steel ratio/ $\%$	Stirrup ratio/ $\%$	Joint forms
CFJ1	C40	0.36	0	4.8	1.26	Middle joint
CFJ2	C40	0.36	50	4.8	1.26	Middle joint
CFJ3	C40	0.36	100	4.8	1.26	Middle joint
CFJ4	C40	0.18	100	4.8	1.26	Middle joint
CFJ5	C40	0.54	100	4.8	1.26	Middle joint
CFJ6	C40	0.18	100	4.8	1.26	Side joint
CFJ7	C40	0.36	100	4.8	1.26	Side joint
CFJ8	C40	0.54	100	4.8	1.26	Side joint

Table 2 Mix ratios of recycled aggregate concrete

RAC strength grade	RCA replacement percentage $r/\%$	Volume per unit volume(kg/m^3)					
		Water cement ratio	Cement	Sand	NCA	RCA	Water
C40	0	0.43	464	585	1187	0	195
	50	0.43	464	585	593.5	593.5	195
	100	0.43	464	585	0	1187	195

Notice: NCA: natural coarse aggregates

developed in this study by using SRRC columns, which are characterized by convenient construction and good mechanical performance of steel beams. It not only exhibits high bearing capacity and good seismic performance, but also has the advantages of simple construction. Therefore, this SRRC column-S beam composite frame joint presents broad application prospects in structural engineering. However, it has been less research on the mechanical properties of composite frame joints, especially the research of seismic damage assessment of the composite frame joints. In fact, the structure under the action of the earthquake will suffer a certain degree of seismic damage due to the plastic deformation, which maybe lead to cause the structural collapse when the seismic damage is very serious (Kostinakis and Morfidis 2017, Song and Guo 2017). In order to evaluate the seismic damage degree of the structures, at present, the damage index (Promis *et al.* 2009, Promis and Ferrier 2012, Yue *et al.* 2016, Desprez *et al.* 2013) is usually used to evaluate the damage degree of the structure after earthquake. In addition, a reasonable and effective calculation model of seismic damage also can accurately reflect the performance levels of structures under different earthquake actions, which can provide the foundation for the structural seismic design and seismic damage assessment.

To evaluate the seismic damage of SRRC column -S beam composite frame joints, we fabricated and tested eight joint specimens of these joints with different axial compression ratios and RCA replacement percentages in

Table 3 Mechanical properties of RAC material

RAC strength grade	RCA replacement percentage $r/\%$	Cube compression strength f_{cu}/MPa	Prismatic axial compression strength f_{cc}/MPa	Tensile strength f_t/MPa	Elastic modulus E_s/MPa
C40	0	45.98	34.94	2.89	2.533×10^4
C40	50	44.46	33.79	2.83	2.508×10^4
C40	100	40.65	30.89	2.67	2.440×10^4

Table 4 Mechanical properties of steel products

Steel type	Yield strength f_y/MPa	Ultimate strength f_u/MPa	Elastic modulus E_s/MPa	Yield strain $\mu_e(10^{-3})$	
Steel in column	flange	329.8	465.8	2.02×10^5	1632
	web	391.5	503	1.99×10^5	1967
Steel beam	flange	268.3	443.6	1.93×10^5	1390
	web	329.8	465.8	2.02×10^5	1632
Longitudinal rebars	$\Phi 14$	446.3	523.8	2.15×10^5	2075
Stirrup	$\Phi 8$	418.9	491.6	2.12×10^5	1976

this paper. The cyclic loading tests of composite frame joints were also carried out. The seismic performance of joints has been analyzed, and the seismic damage model of the joints that can reflect the damage characteristics of the joints was established. In addition, the influence of RCA replacement percentages and axial compression ratio on the seismic damage performance of the joints was also investigated in detail. On the basis of the above results, the relationship among the damage degree, damage level and quantitative index of these joints under the different performance levels was established in this paper. The conclusions can provide a technical reference for the seismic performance design of SRRC column-S beam composite frame joints.

2. Experimental procedures

2.1 Design and manufacture of specimens

Eight SRRC column-S beam composite frame joints were designed and fabricated in this paper, meanwhile, the RCA replacement percentage and axial compression ratio were the design parameters. The main construction details of the joint specimens are presented in Table 1. The section sizes and reinforcements of the joints are shown in Fig. 1. RCA was obtained from waste concrete produced via building demolition, and the basic physical properties of RCA can meet the requirements of "Recycled Coarse Aggregate for Concrete in China (GB/T-25177-2010)". The strength grade of RAC material was taken as C40 and the RAC cover to the outer surface of stirrups was 20 mm. The mixture ratio and mechanical properties of RAC material are shown in Tables 2 and 3, respectively. The welded steel beam and the profile steel in the columns, which was made of Q235 steel, were applied in the specimens. The joints were connected by welding correctly. Steel rebars with a

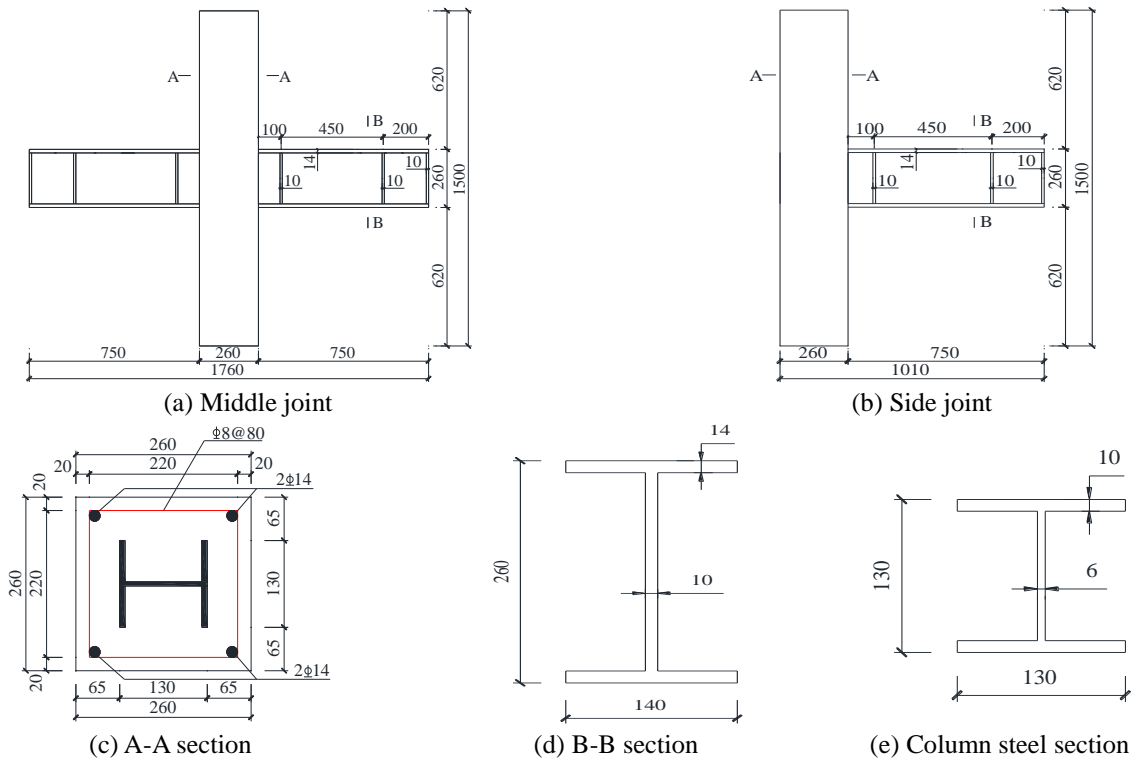


Fig. 1 Design sections sizes and reinforcements of joint specimens



(a) Test loading site

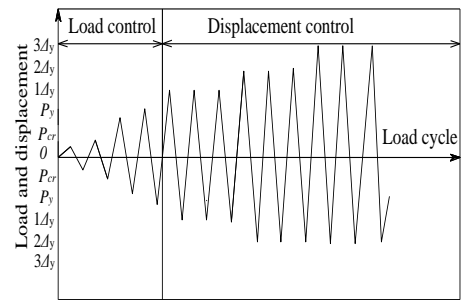
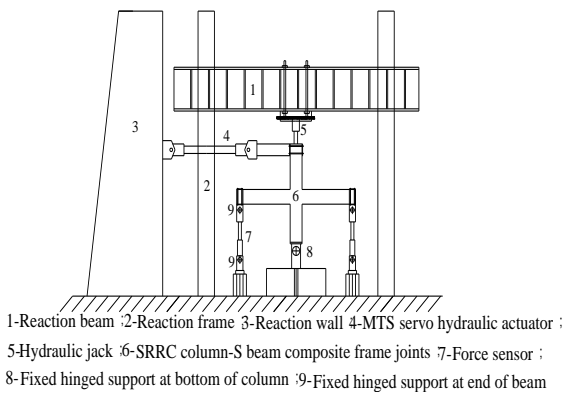


Fig. 3 Loading procedure of joints



(b) Test set-ups

Fig. 2 Test set-ups of joints

diameter of 14 mm were provided for longitudinal reinforcement, and rebars with a diameter of 8 mm and separated by 40 mm were used as transverse stirrups in the joints. Table 4 shows the basic mechanical properties of the steel products.

2.2 Test devices and methods

The cyclic loading tests were conducted on the joints in the structural engineering laboratory of Xi'an University of Technology in West China. The test set-up is illustrated in Fig. 2. All specimens were tested under cyclic lateral loads with the vertical force. The vertical loads were applied by a hydraulic jack before the testing. When the vertical loads reached a stable value, the horizontal cyclic loads were applied to the loading point of columns in the joints by using an electro hydraulic servo test machine. In addition, the lateral loading procedure of the cycle tests included two main steps, namely, a load-controlled step and a displacement-controlled step, as shown in Fig. 3.

Several displacement meters were installed along the surface of the joint specimens to monitor the lateral displacement of the specimens. The strains in the steel flanges, steel webs, longitudinal rebars, and transverse stirrups were measured with strain foils and strain rosettes that were attached to the steel flanges, steel webs, longitudinal rebars and transverse stirrups in advance. The

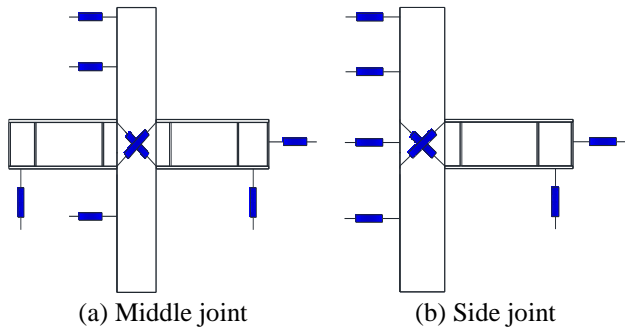


Fig. 4 Test point arrangement of displacement meter in joints

measurement points of the specimens are shown in Figs. 4 and 5.

2.3 Main test process and result analysis

2.3.1 Failure process and failure modes

Experimental observation revealed that the failure processes and modes of the eight joint specimens are similar to each other. CFJ3 specimen is taken as an example to illustrate the failure process of joints in this paper. In the early stage of the loading, no cracks occurred on the specimen surfaces because the deformation of joints was in the elastic stage. With the increase of loads, tiny transverse cracks were observed in the joint regions at the bottom of the steel beam. And the specimens entered the cracking stage. As the magnitudes of the lateral loads increased, diagonal cracks began to appear in the joint core regions, while the original horizontal cracks continued to extend and expand. With the loads increasing, the number of diagonal cracks evidently increased and the original diagonal cracks gradually formed “X” shaped cross diagonal cracks. When the profile steel in the joint regions got into the yielding stage, the displacement cyclic loads was conducted. The length and width of the “X” shaped diagonal cracks increased as the displacement magnitude increased. Meanwhile, the steel webs and stirrups had already yielded. As the loads increased continuously, the “X” shaped diagonal cracks in the joint regions penetrated gradually, and a large part of the recycled concrete of the core area of joints began to crush and fall off. The transverse stirrups yielded and became partly exposed. When the bearing capacity of the specimens decreased to 85% of the peak loads, it indicated that the joints lost their bearing capacity, and the test was stopped. The typical failure modes of these composite joints are shown in Fig. 6.

2.3.2 Hysteresis curves

Fig. 7 shows the load-displacement hysteresis curves of the joints are obtained in the test, and these curves illustrate the relationship between the horizontal loads and the corresponding displacements at the loading point of the frame joints under cyclic loading. The following observations were obtained from Fig. 7.

The hysteresis curves of the specimens were spindle shaped, which shows that the joints possessed good energy dissipation capacity. In the early stage of loading (i.e.;

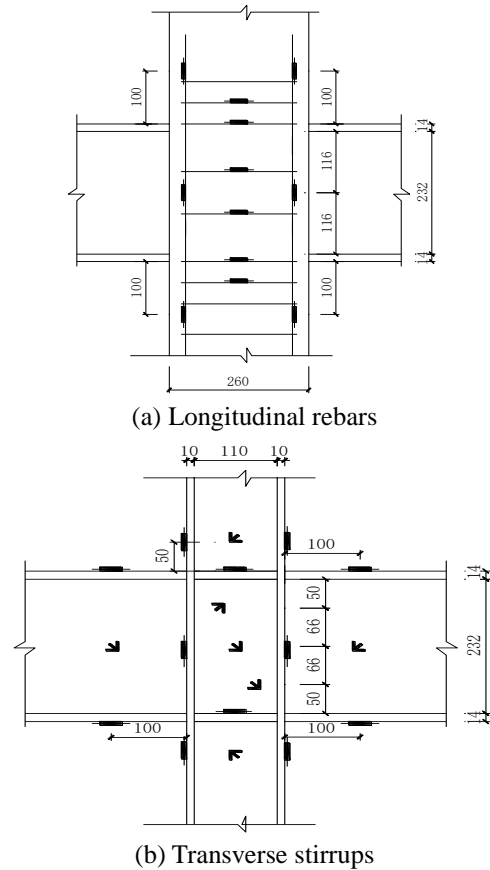


Fig. 5 Strain measuring point arrangement in joints

before cracking), the loads and displacements presented an approximate linear relationship, which indicates that the specimens were basically in an elastic state. In the elastic-plastic state, the cracks occurred on the surface of the joint regions, the slopes of the hysteresis curves began to decrease gradually and residual deformation became relatively obvious. In the displacement-controlled stage, the surrounding area of the hysteresis curves of the joints was enlarged as displacements increased. With regard to the load process at each displacement level, the strength and stiffness of the joints decreased as the number of displacement cycles increased. This type of deterioration mainly reflects damage accumulation in the joints.

The different parameters exerted different influences on the shapes of the hysteresis curves of the joints. Firstly, as the RCA replacement percentage increased, the area inside the hysteresis curves seems to decrease somewhat, indicating that the ductility and energy dissipation capacity of the joints decreased slightly. Secondly, the larger the axial compression ratio is, the smaller the surrounding area of hysteresis curves is. The result indicates that increasing the axial compression ratio is unfavorable to the seismic performance of the frame joints.

In summary, the hysteresis curves of the SRRS column-S beam composite frame joints with different RCA replacement percentages and axial compression ratios under cyclic reverse loading were relatively plump, which shows that the frame joints exhibit good seismic performance with a reasonable design.

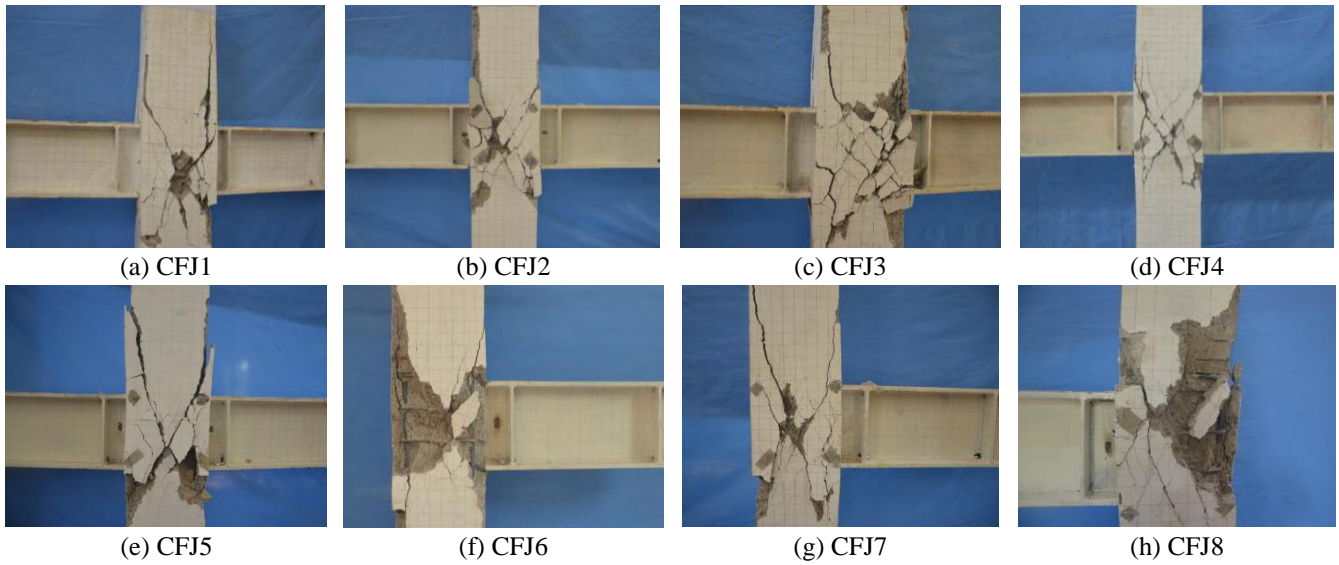


Fig. 6 Failure patterns of joint specimens

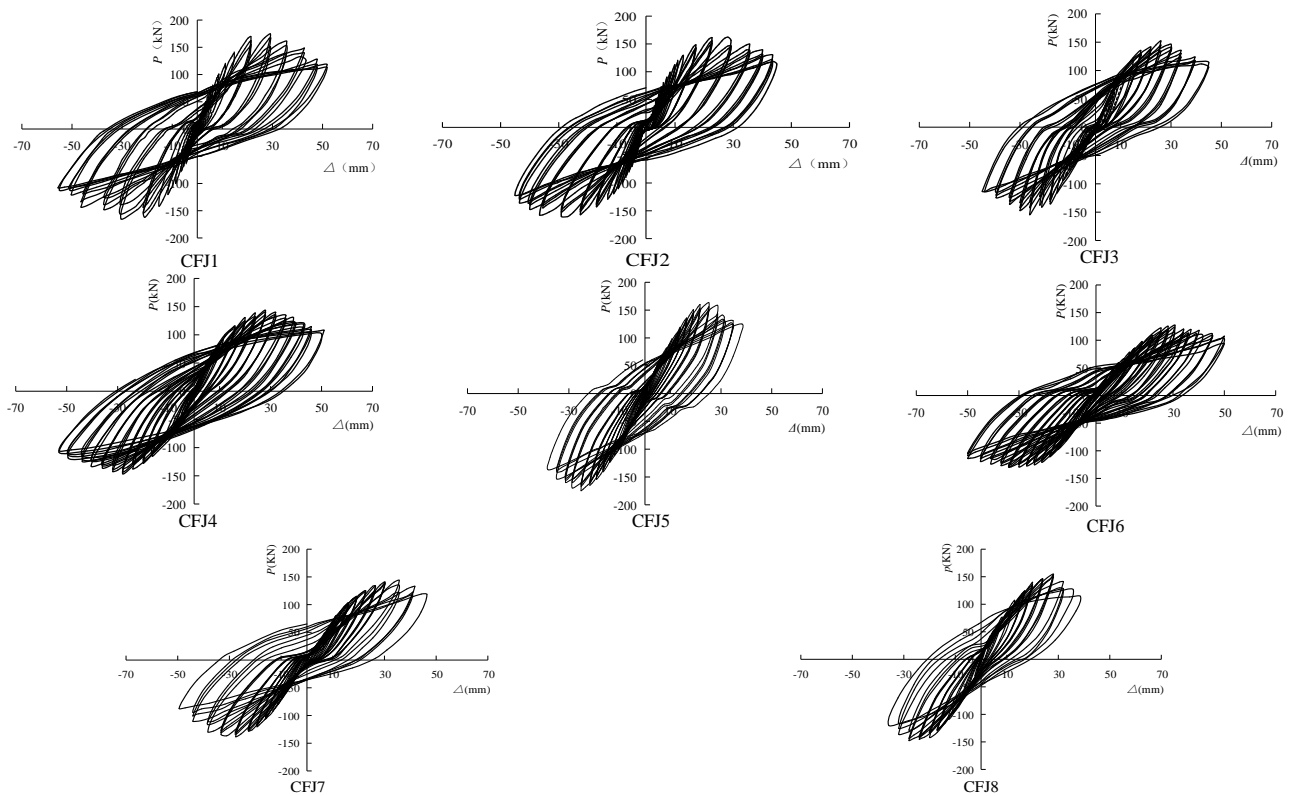


Fig. 7 Load-displacement hysteresis curves of joints

Table 5 lists the measured crack loads, yield loads, maximum loads, and ultimate loads of the joints (P_{cr} , P_y , P_m and P_u , respectively). Table 6 summarizes the deformation features of the joints, including crack, yield, peak and ultimate displacements (Δ_{cr} , Δ_y , Δ_m and Δ_u , respectively) corresponding to the characteristic loads of the joints. In addition, the ductility coefficient μ of the joints can be defined as the ratio of ultimate displacement to yield displacement and is also presented in Table 6. Tables 5 and 6 indicate that the ductility coefficient and cumulative energy consumption of the joints presented a decreasing

trend with the increase in RCA replacement percentage and axial compression ratio. Meanwhile, the mean value of the ductility coefficient of the joints was 3.207, which can meet seismic requirements and indicate a good energy dissipation capacity. By the way, the influence law of cumulative hysteretic energy is also consistent with the ductility of the joints, which can both reasonably reflect the seismic performance of the joints.

3. Calculation on damage indexes

Table 5 Characteristic loads and cumulative energy dissipation of joints

Specimen No	Push loads				Pull loads				Cumulative energy dissipation kN·mm
	P_{cr}^+ /kN	P_y^+ /kN	P_{max}^+ /kN	P_u^+ /kN	P_{cr}^- /kN	P_y^- /kN	P_{max}^- /kN	P_u^- /kN	
CFJ1	73.2	130.24	175.1	148.8	-71.51	-132.05	-165.57	-140.73	10648.367
CFJ2	68.6	118.54	163.17	137.9	-70.12	-125.06	-161.1	-136.94	10525.149
CFJ3	65.0	112.06	152.13	129.31	-67.0	-115.27	-154.24	-131.1	10308.442
CSJ4	52.13	91.29	143.23	121.75	-54.62	-92.36	-146.49	-124.52	11901.604
CSJ5	74.0	107.86	163.24	138.75	-71.21	-109.67	-174.61	-148.42	8812.854
CSJ6	50.01	82.37	127.14	108.07	-52.31	-95.16	-130.21	-110.68	10811.579
CSJ7	51.23	94.31	143.91	122.32	-55.23	-96.82	-138.15	-117.43	9343.940
CSJ8	60.23	108.26	154.4	131.24	-65.42	-107.86	-147.29	-125.2	8072.217

Table 6 Characteristic displacements and ductility coefficient of joints

Specimen No	Push displacements				Pull displacements				Ductility coefficient $\mu=\Delta_u/\Delta_y$
	Δ_{cr}^+ /mm	Δ_y^+ /mm	Δ_{max}^+ /mm	Δ_u^+ /mm	Δ_{cr}^- /mm	Δ_y^- /mm	Δ_{max}^- /mm	Δ_u^- /mm	
CFJ1	5.57	13.05	26.7	42.67	-5.62	-13.37	-27.38	-46.65	3.379
CFJ2	5.16	12.43	28.31	39.91	-5.03	-13.15	-29.03	-42.73	3.230
CFJ3	5.47	12.67	26.94	39.01	-5.7	-13.21	-27.61	-42.01	3.130
CSJ4	6.23	12.60	31.68	47.61	-6.7	-13.37	-33.15	-52.15	3.838
CSJ5	7.45	12.57	25.32	33.65	-7.26	-11.92	-25.67	-36.23	2.858
CSJ6	7.32	13.67	30.79	47.85	-7.64	-14.49	-32.86	-52.47	3.561
CSJ7	7.23	14.29	34.97	43.86	-7.85	-14.12	-28.59	-42.79	3.050
CSJ8	6.56	13.64	27.89	34.98	-6.74	-13.15	-27.01	-35.01	2.613

The damage indexes (Kappos 1997) of structures generally provide a certain numerical indication that can be used to assess the evolution of the damage behavior of structures. Different damage indexes for structural properties have been proposed in literatures, and these include strain, displacement, stress, strength, dissipated energies, stiffness and dynamic properties (Banon and Veneziano 1982, Stephens and Yao 1987, Gosain *et al.* 1977, Meyer *et al.* 1988). All these damage indexes can be categorized into two namely, the cumulative and non-cumulative indexes. The cumulative indexes usually measure the damage of structures on the basis of loading amplitude and number of loading cycles. In addition, the non-cumulative indexes are calculated with the maximum mechanical parameters such as displacement, rotation and curvature. The descriptions of the main calculation methods and models of damage indexes for structures are explained below.

3.1 Index based on displacement

The typical calculation method of damage index based on the maximum displacement of structures has been described in literature (Banon and Veneziano 1982, Stephens and Yao 1987). The first term D_1 expresses the linear cumulative of damage. The expression of first term D_1 is calculated as follows

$$D_1 = \frac{e^{n\beta_w} - 1}{e^n - 1} \quad (1)$$

In addition, the cumulative term β_w is calculated

$$\beta_w = c \sum_i \frac{\delta_i}{\delta_f} \quad (2)$$

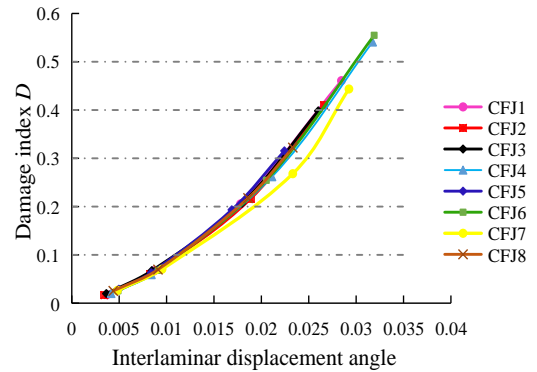


Fig. 8 Damage index of joints based on displacement

Where δ_i is the maximum displacement for a cycle, δ_f is the displacement of destruction state in monotonous loading; and $c=0.1$. When the joint is strengthened, $n=1$; otherwise, $n=-1$.

The second term D_2 is calculated by the sum of the ratios of plastic displacement

$$D_2 = \sum_i \left(\frac{\Delta\delta_+}{\Delta\delta_f} \right)^{1.77} \quad (3)$$

Where $\Delta\delta_+$ is the positive increment of the plastic displacement, and $\Delta\delta_f$ is 10% of the height of the construction H .

Fig. 8 shows the evolution process of seismic damage indexes of joints calculated by the maximum displacement. As shown in Fig. 8, the development laws of the damage indexes of joints are similar considerably. In particular, specimens CFJ5 and CFJ8 with a large axial compression ratio present poor ductility, which leads to the faster

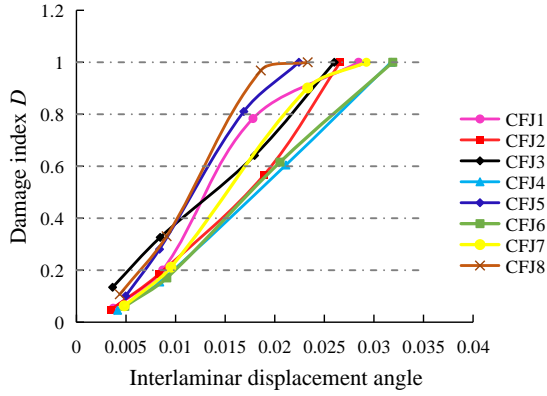


Fig. 9 Damage index of joints based on energy

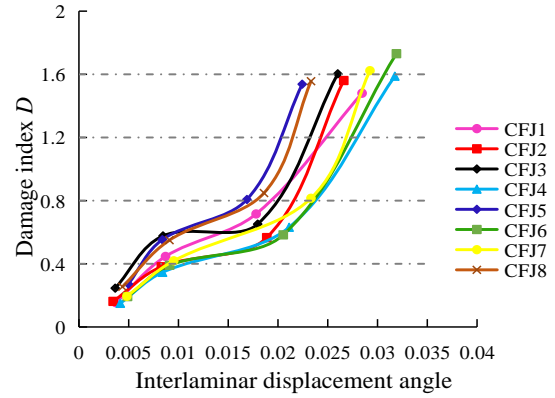


Fig. 10 Damage index of joints based on Park-Ang model

development rate of the seismic damage of the joints. On the contrary, specimens CFJ4 and CFJ6 with a small axial compression ratio present better ductility, and development rate of damage is relatively slow. However, an almost linear relationship is observed between the damage index and displacement angle, which is inconsistent with the damage process of the joints. Therefore, the damage index based on the maximum displacement cannot fully reflect the development process of the seismic damage of joints.

3.2 Index based on energy

Previous studies (Gosain *et al.* 1977, Meyer *et al.* 1988) have proposed a calculation formula of the damage index based on the energy absorbed in the hysteresis loops. The typical Eq. (4) consists of the ratio between dissipated energy during each loading cycle and the total dissipated energy of the structures.

$$D = \sum_i \frac{\int dE}{E} \quad (4)$$

Fig. 9 presents the evolution of damage indexes expressed in terms of dissipated energy. The damage curves are basically similar to each other, but the slopes of the curves are slightly different. In the same displacement condition, the damage indexes of CFJ4 and CFJ6 are clearly lower than those of the other specimens, and those of CFJ5 and CFJ8 are higher than those of the other specimens. This result can be explained by that the greater the axial compression ratio is, the faster the seismic damage develops. However, the damage curves do not show the steady development process of joint failure, which is different from the experimental process. Therefore, the damage index based on dissipated energy cannot rationally reflect the development process of the seismic damage of joints.

3.3 Combined indexes

(1) Park-Ang damage model

Experimental investigations of structural members and structures have indicated that excessive deformation and hysteretic energy are the most important factors that contribute to the seismic damage. Therefore, the seismic

damage models that combine the maximum deformation and hysteretic energy are more reasonable. One of the well-known and widely used cumulative damage models is the Park-Ang model (Park and Ang 1985), which is expressed as follows

$$D = \frac{\delta_m}{\delta_u} + \beta \frac{E_h}{F_y \delta_u} \quad (5)$$

Where δ_m is the maximum deformation for a cycle, δ_u is the ultimate deformation under monotonic loading, F_y is the yield strength, E_h is the cumulative hysteretic energy; and β is an experimental coefficient to estimate the energy contribution, and $\beta=0.25$ can be used for slightly reinforced structures.

The combined index Eq. (5) based on the Park-Ang model involves displacement and dissipated energy which is overvalued by the calibration term β . This index combines the brittle failure of concrete with the ductile failure of steel. The first term δ_m/δ_u represents normalized displacement. The second term $E_h/F_y\delta_u$ is the dissipated energy standardized by cumulative energy corresponding to the product of the steel yielding load and the displacement required to reach failure.

Fig. 10 presents the evolution of the damage index obtained with the Park-Ang seismic damage model. The damage process of the frame joints expressed by the comprehensive consideration of displacement and energy dissipation is more reliable and reasonable than that of the single displacement or cumulative energy. However, the Park-Ang damage model does not converge at its upper limits according to Fig. 10. For example, the damage index exceeds 1.0 when the structures are loaded monotonically to failure.

(2) Modified Park-Ang damage model

Given this issue, the objective of this paper is to develop a modified Park-Ang damage model in which the non-convergence problem at upper limits does not exist. Furthermore, the seismic performance levels of joints are quantified with the modified model by setting a certain limit value of the damage indexes.

This work correctly identified the relationship between deformation damage component D_δ and energy dissipation component D_e by introducing combination coefficient α .

Table 7 Combination coefficient α value of joints

Joint specimens	CFJ1	CFJ2	CFJ3	CFJ4	CFJ5	CFJ6	CFJ7	CFJ8
Push loads	0.0022	0.0054	0.0153	0.0703	0.0721	0.0374	0.0742	0.0352
Pull loads	0.0098	0.0892	0.0714	0.1262	0.1425	0.0529	0.0399	0.0367

This coefficient addresses the convergence problem of the damage model at the upper boundary. The equation of the modified Park-Ang damage model can be expressed as follows

$$D_{P-A}^M = (1 - \alpha) D_\delta + \alpha D_e \quad (6)$$

In Eq. (6), the damage D_δ of deformation component and the damage D_e of energy consumption component are listed respectively.

$$D_\delta = \frac{\delta_m - \delta_y}{\delta_u - \delta_y} \quad (7)$$

$$D_e = \frac{E_h}{F_y \delta_u} \quad (8)$$

Taking the Eq. (7) and Eq. (8) into Eq. (6), the modified Park-Ang damage model of composite frame joints can be expressed as follows

$$D_{P-A}^M = (1 - \alpha) \frac{\delta_m - \delta_y}{\delta_u - \delta_y} + \alpha \frac{E_h}{F_y \delta_u} \quad (9)$$

Strictly speaking, when the structure is not damaged, $D_{P-A}^M = 0$; When the structure is completely destroyed, $D_{P-A}^M = 1$; When $0 < D_{P-A}^M < 1$, the structure is in a state between no damage and complete damage. In order to make the modified model converge on the boundary conditions, the combination coefficient α is derived by the numerical inversion method, which is based on the condition of damage index $D=1.0$; and then inversely deduce the expression of combination coefficient α .

$$\alpha = \frac{F_y \delta_u (\delta_u - \delta_m)}{E_h (\delta_u - \delta_y) - F_y \delta_u (\delta_m - \delta_y)} \quad (10)$$

With the test investigation results, combination coefficient α under push and pull loads is calculated and is shown in Table 7. The mean value of α derived by Eq. (10) is 0.055, and the standard deviation is 0.0397. The coefficient of variation (COV) reaches 72.1%, which implies the complexity of the damage behavior of composite frame joints.

SPSS is a software of statistical products and service solutions. In this paper, SPSS software is used to fit the multivariate linear equation of combination coefficient α , which is based on RCA replacement percentage r and axial compression ratio n . The calculation formula of α can be expressed as follows

$$\alpha = -0.005 + 0.055r - 0.003n \quad (11)$$

In addition, the damage index D is normalized by the above-mentioned combination coefficient α . The formula is

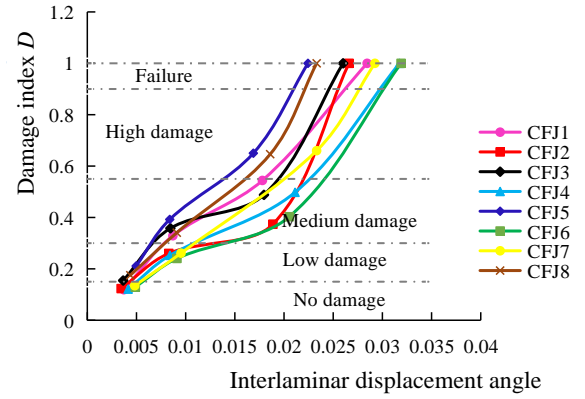


Fig. 11 Damage index of joints based on modified Park-Ang model

as follows

$$D_n = \frac{D_i}{D_u} \quad (12)$$

Where D_n is the normalized damage index; D_i is the damage index calculated through main characteristic loads, respectively; D_u is the damage index of the ultimate state. D_i is the damage index corresponding to each characteristic point; and D_u is the damage index under the limit state.

Fig. 11 illustrates the development process of the damage of the joints is based on the modified damage model. The seismic damage of frame joints is a relatively stable development process. In the beginning of loading, the destruction process and damage development of joints are relatively slow. As the loads increased, the cracking of joints is becoming more and more serious, and causes the development rate of damage to increase quickly. The modified damage model can address the convergence problem of the Park-Ang model in the upper bounds, and can reflect the damage development process of this type of composite frame joints.

4. Analysis on seismic damage of the joints

4.1 Damage process of the joints

According to the calculation results of the seismic damage of the joints, the seismic damage process of the joints under cyclic loading can be divided into the following five main stages:

(1) No damage stage

In the beginning of loading, no obvious phenomenon was observed in the joints. The joints were in the elastic stage, and the deformation of the joints could be restored completely. The strain of transverse stirrups, longitudinal rebars and profile steel was really very small. At this stage, the joints were in a very good working condition and the damage index was within 0.15.

(2) Initial damage stage

With the increase in loads, the horizontal cracks

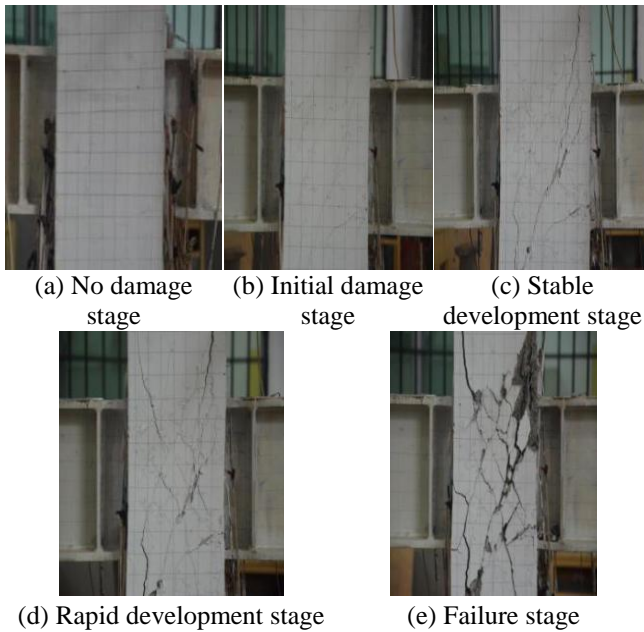


Fig. 12 Typical damage process of CFJ3 joint

gradually appeared on the surface of RAC, and the joints began to enter the cracking stage. The strain of the stirrups, longitudinal rebars and profile steel gradually increased. At this stage, the shear force of joints was mainly borne by recycled concrete, and the damage index of joints at this moment was approximately 0.3.

(3) Stable development stage of damage

As the load continued to increase, diagonal cracks began to appear in the core area of joints, and the original cracks continued to extend. Meanwhile, the steel web began to yield gradually and the strain of the stirrups increased rapidly until yielding. At this stage, the shear force of the joints was borne by the steel web and stirrups. The damage index of the joints in this state was approximately 0.55.

(4) Rapid development stage of damage

As the loads increased, the core region of the joints began to form cross diagonal cracks and continued to extend and expand. When the peak load was reached, the cross diagonal cracks gradually penetrated. At the same time, a small piece of recycled concrete fell off in the core area of joints accompanied with a tearing sound of recycled concrete. At this point, the joints exhibited large residual strain, and the damage index of the joints was about 0.9.

(5) Failure stage

After the peak load, RAC in the region of the joints continued to fall off, and the stirrups yielded and became partly exposed. When the bearing capacity of the joints decreased to 85% of the peak load, the strength and stiffness of joints were drastically reduced, and the joints failed; this condition indicates that the joints had lost their bearing capacity. At this stage, the damage index was taken as 1.0.

In summary, the seismic damage of the frame joints exhibited a gradual evolutionary process as the cyclic loads

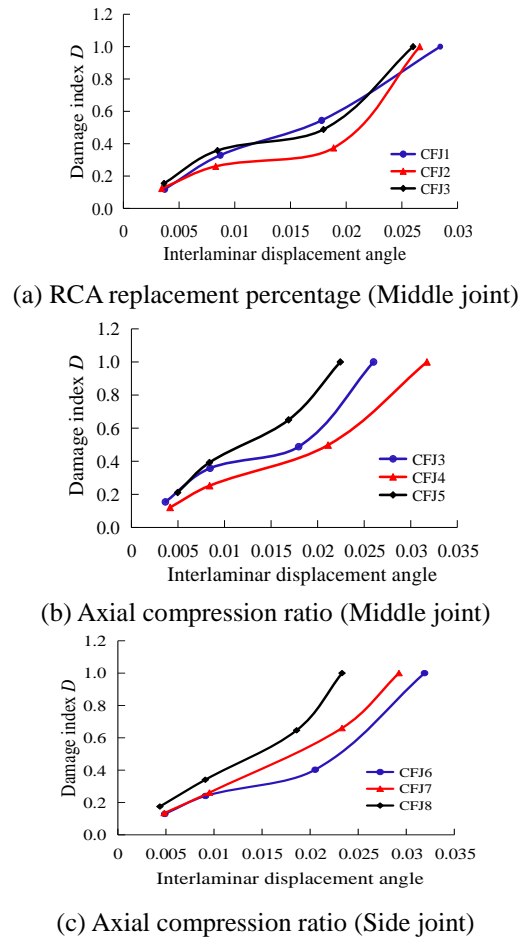


Fig. 13 Influence of design parameters on the damage indexes of joints

increased. Fig. 12 indicates the typical damage process of CFJ3 joint at different load stages during the cyclic test.

4.2 Influence of parameters on damage

According to the calculation results of the damage indexes of joints, it can be seen that RCA replacement percentage and axial compression ratio both have a certain adverse influence on the development law of the seismic damage of joints, as shown in Fig. 13.

Fig. 13(a) indicates that the damage index is small in the beginning of loading and the RCA replacement percentage has little effect on the damage development of the joints. As the loads increased, the joints began to break, and the strain of transverse stirrups, longitudinal rebars and profile steel increased dramatically. The value of the seismic damage index of the joints also increased rapidly.

The effects of axial compression ratio on the damage development of the frame joints are shown in Figs. 13(b) and 13(c). The damage indexes of the joints developed rapidly as the axial compression ratio increased. That is, a large axial compression ratio equated to a large damage index value mainly because the frame joints with relatively high axial compression ratios possess poor ductility deformation capability, which leads to the rapid development of seismic damage.

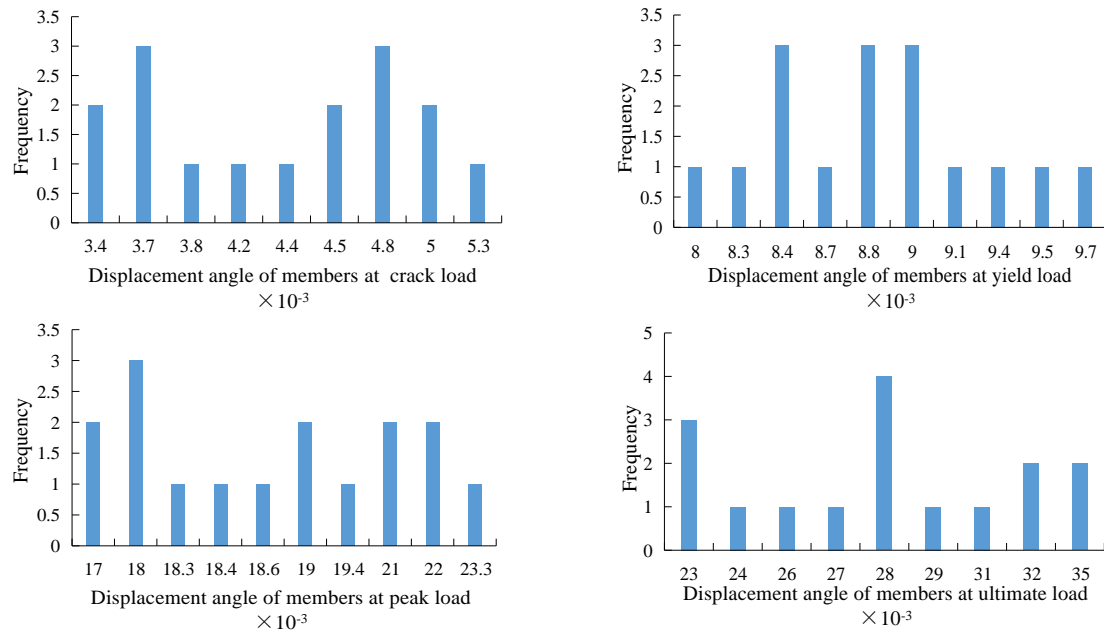


Fig. 14 Statistical results of displacement angle for the characteristic loads of joints

Table 8 Seismic damage performance and damage index of composite frame joints

Performance level	Damage level	Repairable degree	Limit values of displacement angle	Damage index
Normal use	Basically good	No repair required	1/260	0-0.15
Temporary use	Slight damage	Possible repair	1/120	0.15-0.3
Repair after use	Moderate damage	Minimal repair	1/60	0.3-0.55
Life safety	Serious damage	Need repair	1/45	0.55-0.9
Collapse prevention	Collapse	Non repairable	1/35	0.9-1.0

5. Seismic performance levels and quantitative indexes of joints

According to relevant regulations of “*general rule for performance-based seismic design of buildings*” in China (CECS 160 2004), the seismic performance levels of the joints can be divided into five categories: normal use, temporary use, repair after use, life safety and collapse prevention. In addition, the displacement angle is used as the quantification index of the seismic performance level of the frame joints in this study. Interlaminar displacement angle is the ratio of the maximum horizontal displacement to the height of the floor. The main purpose is to limit the horizontal displacement of the structure under normal service conditions, and ensure the stiffness, bearing capacity, stability and operation requirements of the structure. According to CECS 160: 2004 in China, the probability reliability of the guarantee rate is 84.13% for the structures, and this value is obtained by subtracting the standard deviation from the mean value, which is in line with GB 50223-2008 provisions (Liu *et al.* 2010, GB 50223 2008). It can meet the current standards of construction

industry in China. In addition, the characteristic points of the frame joints were made to correspond to different seismic damage levels, that is, the crack load corresponded to the basically good state, the yield load corresponded to the slight damage state, the peak load corresponded to the medium failure state, while the ultimate load corresponded to the serious damage state. Fig. 14 shows the statistical results of the displacement angle of these frame joints by the test load characteristic points. Based on Fig. 14, the following results were obtained:

(1) When the recycled concrete frame joint entered the cracking state, the displacement angle changed from 1/298 to 1/188, with an average value of 1/222 and a standard deviation of 1/1578. When the probability guarantee rate of the joints is 84.13%, the displacement angle is 1/258. In order to meet the seismic fortification requirements of “No bad under small earthquake”, the 1/260 can be used as the value of elastic displacement angle under the condition of “basically good” state.

(2) In the yield state, the displacement angle of the joints was between 1/126 and 1/104. Meanwhile, the average value and standard deviation are 1/113 and 1/2198, respectively. When the probability guarantee rate is 84.13%, the displacement angle is 1/119. Combined with the standard of seismic strengthening and identification existing in relevant codes GB 50223-2008 and GB 50023-2009, 1/120 was taken as the value of elastic displacement angle under the “slight damage” level.

(3) When the peak load of the joints was reached, the displacement angle of the joints was between 1/59 and 1/43, with an average value of 1/52 and a standard deviation of 1/632. When the probability guarantee rate is 84.13%, the displacement angle of the joints was 1/57. To meet the seismic fortification standard of “Repairable under Moderate Earthquake”, the 1/60 was used as the elastic displacement angle value under the “moderate damage” level.

(4) After the peak loads, the displacement angle of the joints changed from 1/45 to 1/29, with an average value of 1/35 and a standard deviation of 1/264. When the probability guarantee rate of joints is 84.13%, the displacement angle is 1/40. To ensure the safety of people's lives and property, it is necessary to consider a certain security reserve. Thus, the elastic displacement angle value under the "serious damage" state was about 1/45.

(5) According to the definition of the collapse boundary in previous literature (Gao and Bao 1985), the value of the displacement angle of joints can be taken as 1/35.

Based on the above results, Table 8 shows the relationship among seismic performance level, damage level and damage index of SRRC column-S beam composite frame joints.

6. Conclusions

The seismic damage of the joints was evaluated and analyzed by studying the seismic performance of eight SRRC column-S beam composite frame joints. The main conclusions are as follows:

- The seismic performance level of composite frame joints can be divided into five grades, namely normal use, temporary use, repair after use, life safety and collapse prevention.
- With the displacement angle as the quantitative index, the values of joints under different earthquake were given by means of mathematical statistics. The values were 1/260, 1/120, 1/60, 1/45 and 1/35 corresponding to crack load, yield load, peak load, ultimate load and the definition of the collapse boundary, respectively.
- A modified Park-Ang damage model was established, and the expression of coefficient α was derived by using SPSS software. RCA replacement percentage exerted little influence on the damage process of the joints. In addition, the axial compression ratio was disadvantageous to the damage development of the joints.
- The range of the damage index of composite frame joints under different performance levels was determined. Meanwhile, the relationship among the performance level, damage level and damage index of the joints was established, which can provide some references for the seismic evaluation.
- Although the results are good, the conclusions cannot be widely applied due to the less experimental data. Moreover, the model needs to be further improved.

Acknowledgments

The research was financially supported by the National Natural Science Foundation of China P.R. (No. 51408485), China Postdoctoral Science Foundation Funded Project (No. 2015M572584), the Plan Projects of the Department of Housing and Urban-rural Development of Shaanxi Province (No. 2015-K129), Shaanxi Province Postdoctoral Science Foundation Funded Project, the Project Supported by Natural Science Basic Research Plan in Shaanxi Province of

China (No. 2016JQ5024), which is gratefully acknowledged.

References

- Banon, H. and Veneziano, D. (1982), "Seismic safety of reinforced concrete members and structures", *Earthq. Eng. Struct. Dyn.*, **10**, 179-93.
- Carneiro, J.A., Lima, P.R.L. and Leite, M.B. (2014), "Compressive stress-strain behavior of steel fiber reinforced-recycled aggregate concrete", *Cement Concrete Compos.*, **46**(2), 886-893.
- Choi, W.C. and Yun, H.D. (2012), "Compressive behavior of reinforced concrete columns with recycled aggregate under uniaxial loading", *Eng. Struct.*, **41**(8), 285-293.
- Desprez, C., Mazars, J., Kotronis, P. and Paultre, P. (2013), "Damage model for FRP-confined concrete columns under cyclic loading", *Eng. Struct.*, **48**(3), 519-531.
- Gao, X.W. and Bao, A.B. (1985), "Probability model of seismic action and its statistical parameters", *Earthq. Eng. Eng. Vib.*, **5**(1), 13-22.
- GB 50023 (2009), Standard for Seismic Appraisal of Buildings, State Standard of the People's Republic of China, Beijing, China.
- GB 50223 (2008), Standard for Classification of Seismic Protection of Building Constructions, State Standard of the People's Republic of China, Beijing, China.
- Gosain, N.K., Brown, R.H. and Jirsa, J.O. (1977), "Shear requirements for load reversal on reinforced concrete members", *Earthq. Eng.*, **103**(7), 1461-76.
- Kappos, A.J. (1997), "Seismic damage indices for RC buildings: evaluation of concepts and procedures", *Prog. Struct. Eng. Mater.*, **1**(1), 78-87.
- Kostinakis, K. and Morfidis, K. (2017), "The impact of successive earthquakes on the seismic damage of multistorey 3D R/C buildings", *Earthq. Struct.*, **12**(1), 1-12.
- Kou, S.C., Poon, C.S. and Wan, H.W. (2012), "Properties of concrete prepared with low-grade recycled aggregates", *Constr. Build. Mater.*, **36**(11), 881-889.
- Kumar, R. (2017), "Influence of recycled coarse aggregate derived from construction and demolition waste (CDW) on abrasion resistance of pavement concrete", *Constr. Build. Mater.*, **142**(7), 248-255.
- Leiva, C., Guzmán, J.S. and Marrero, M. (2013), "Recycled blocks with improved sound and fire insulation containing construction and demolition waste", *Waste Manage.*, **33**(3), 663-671.
- Liu, Y., Guo, Z.X. and Huang, Q.X. (2010), "Experimental study of damage model for SRC columns", *J. Wuhan Univ. Technol.*, **32**(9), 203-207.
- Ma, H., Xue, J.Y. and Zhang, X.C. (2013), "Seismic performance of steel-reinforced recycled concrete columns under low cyclic load", *Constr. Build. Mater.*, **48**(11), 229-237.
- Manzi, S., Mazzotti, C. and Bignozzi, M.C. (2013), "Short and long-term behavior of structural concrete with recycled concrete aggregate", *Cement Concrete Compos.*, **37**(3), 312-318.
- Mas, B., Cladera, A., Olmo, T.D. and Pitarch, F. (2012), "Influence of the amount of mixed recycled aggregates on the properties of concrete for non-structural use", *Constr. Build. Mater.*, **27**(1), 612-622.
- Matar, P. and Dalati, R.E. (2011), "Strength of masonry blocks made with recycled concrete aggregates", *Phys. Procedia*, **21**, 180-186.
- Meyer, I.F., Wratzig, W.B. and Stangenberg, F. (1988), "Damage prediction in reinforced concrete frames under seismic action", *Eur. Earthq. Eng.*, **2**(3), 9-15.
- Park, Y.J. and Ang, H.S. (1985), "Mechanistic seismic damage

- model for reinforced concrete”, *J. Struct. Eng.*, ASCE, **111**(4), 722-739.
- Promis, G. and Ferrier, E. (2012), “Performance indices to assess the efficiency of external FRP retrofitting of reinforced concrete short columns for seismic strengthening”, *Constr. Build. Mater.*, **26**(1), 32-40.
- Promis, G., Ferrier, E. and Hamelin, P. (2009), “Effect of external FRP retrofitting on reinforced concrete short columns for seismic strengthening”, *Compos. Struct.*, **88**(3), 367-379.
- Radonjanin, V., Malesev, M. and Marinkovic, S. (2013), “Green recycled aggregate concrete”, *Constr. Build. Mater.*, **47**(10), 1503-1511.
- Silva, R.V., Brito, J.D. and Evangelista, L. (2016), “Design of reinforced recycled aggregate concrete elements in conformity with Eurocode 2”, *Constr. Build. Mater.*, **105**(2), 144-156.
- Song, L.L. and Guo, T. (2017), “Probabilistic seismic performance assessment of self-centering prestressed concrete frames with web friction devices”, *Earthq. Struct.*, **12**(1), 109-118.
- Stephens, J.E. and Yao, J.T.P. (1987), “Damage assessment using response measurements”, *Struct. Eng.*, **113**(4), 787-801.
- Thomas, C., Setién, J. and Polanco, J.A. (2013), “Durability of recycled aggregate concrete”, *Constr. Build. Mater.*, **40**(3), 1054-1065.
- Wagih, A.M., El-Karmoty, H.Z. and Ebid, M. (2013), “Recycled construction and demolition concrete waste as aggregate for structural concrete”, *HBRC J.*, **9**(3), 193-200.
- Xiao, J.Z., Li, W.G., Fan, Y.H. and Huang, X. (2012), “An overview of study on recycled aggregate concrete in China (1996-2011)”, *Constr. Build. Mater.*, **31**(6), 364-83.
- Xue, J.Y., Bao, Y.Z. and Ren, R. (2014), “Experimental study on seismic behavior of steel reinforced concrete frame joints under low cyclic reversed loading”, *J. Civil Eng.*, **47**(10), 1-8.
- Yue, J.G., Qian, J. and Beskos, D.E. (2016), “A generalized multi-level seismic damage model for RC framed structures”, *Soil Dyn. Earthq. Eng.*, **80**(1), 25-39.